



ON THE EFFECTS OF CRACKS WITHIN SACRIFICIAL BED MATERIAL ON THE GROWTH OF MOLTEN POOLS

R S PECKOVER
J H ADLAM
B D TURLAND

CULHAM LABORATORY
Abingdon Oxfordshire

1978

This document is intended for publication in a journal or at a conference and is made available on the understanding that extracts or references will not be published prior to publication of the original, without the consent of the authors.

Enquiries about copyright and reproduction should be addressed to the Librarian, UKAEA, Culham Laboratory, Abingdon, Oxon. OX14 3DB, England.

ON THE EFFECTS OF CRACKS WITHIN SACRIFICIAL BED MATERIAL ON THE GROWTH OF MOLTEN POOLS

R S Peckover, J H Adlam and B D Turland

UKAEA Culham Laboratory, Abingdon, Oxon. OX14 3DB, UK

ABSTRACT

When a liquid with internal heat sources is present in a cavity in a solid substrate and has a temperature higher than the melting point of the solid, the pool may grow by melting the cavity boundary. If the substrate contains fissures then the molten material can penetrate down these ahead of the main melting front. Wide cracks will be enlarged by further melting. A critical fissure size has been calculated, such that if a crack is narrower than the critical width, it will not be enlarged by melting and the penetration by molten material ahead of the main melting front will be arrested. Thermal stresses induced in the solid ahead of the melting front may produce fissures in brittle poorly conducting materials. A criterion determining when thermal shock fragmentation is likely to be important in this context is developed.

(Paper presented at Fourth Post Accident Heat Removal Conference, Ispra Joint Research Centre, 10th - 13th October, 1978).

On the effects of cracks within sacrificial bed material on the
growth of molten pools

Peckover R S, Adlam J H and Turland B D
UKAEA Culham Laboratory, Abingdon, Oxon, U.K.

1. INTRODUCTION

The use of a bed of sacrificial material beneath the primary vessel of a nuclear reactor is currently being evaluated as a possible additional containment barrier to arrest the downward motions of molten core debris in the hypothetical event of a whole core melt-down. Such a bed, made of a highly refractory material such as alumina, and miscible with the oxide phase of the core debris, has been considered in calculations of the growth of a molten pool on the assumption that the bed forms a smooth continuum[1]. The stability of the melting front to spatial perturbations has been examined [2] and for small amplitude perturbations the melting front has been found to be stable in shape, and the assumption for deep pools that the melting front is a smooth curve justified. However in practice the bed may consist of loose filler or be constructed of blocks, fitted together. Moreover, sudden contact by hot molten core debris will induce thermal stresses with the bed material, and, for brittle poorly conducting materials, can result in further fragmentation. Based on rather simple modelling, a criterion for when thermal shock fragmentation is likely to be important is developed. The molten core debris can then penetrate to some extent down the resulting fissures in advance of the main melting front as the pool grows and is diluted by sacrificial material. Estimates are presented of critical fissure dimensions for different shapes of fissure such that if a crack is narrower than critical then it will not be enlarged by melting, and the penetration by a finger of molten core debris will be arrested.

2. FISSURE PRODUCTION

We wish to estimate whether cracking of solid rock ahead of an advancing melting front is likely to occur, and whether, if a sacrificial bed composed of blocks is incorporated, the blocks are likely to be broken into fragments by thermal stress prior to the arrival of the melting front.

The stresses induced in a body by a temperature difference ΔT across it depend on the geometric shape of the body, the presence of pre-existing cracks, the external constraints and the form of the stress-strain relationship. A characteristic thermal stress for an elastic body is given by

$$\tau_0 = E \alpha \Delta T / (1 - \nu) \quad (2.1)$$

where E is Young's modulus of elasticity, α is the temperature coefficient of linear expansion and ν Poisson's ratio. The stress tensor can then be represented by $\underline{\tau} = \tau_0 \underline{\Gamma}$ where the tensor $\underline{\Gamma}$ is dimensionless and its components are essentially shape factors, which are functions of position and time.

For a thin spherical shell with a flow of heat from the interior to the exterior there is a compressive tangential stress of $\frac{1}{2}\tau_0$ at the inner surface and a tensile tangential stress of the same magnitude at the outer surface. The radial stress is much less than the tangential stress, for a thin shell. If we consider basalt, then for Dresser basalt, which has a tensile strength σ_t of $3 \times 10^7 \text{ N/m}^2$ we may take $E = 10^{11} \text{ N/m}^2$, $\alpha = 10^{-5} \text{ K}^{-1}$, $\nu = 0.25$. This gives τ_0 the value $\sim (4/3) 10^6 (\Delta T) \text{ N/m}^2$. Thus the basalt will fail in tension for a temperature difference

(ΔT) of 50K. This assumes that the basalt is perfectly brittle; if there is any non-linearity or plastic deformation before failure, then a larger temperature difference is required to produce cracking.

A molten pool produced in rock or a concrete basemat may be considered as a hot liquid in a thick-walled crucible. Let us consider a thick spherical shell of inner radius r_i and outer radius r_o (fig.1). In spherical co-ordinates (r, θ, ϕ) with spherical symmetry, the radial stress is given by ([3], p420)

$$\tau_{rr} = \frac{2}{3}\tau_o(1-[r_i/r]^3)(\bar{T}(r_o)-\bar{T}(r)) \quad (2.2)$$

when $\tau_{rr}=0$ on both surfaces of the shell, and the tangential stress $\tau_{\theta\theta}$ (which is equal to $\tau_{\phi\phi}$) is

$$\tau_{\theta\theta} = \tau_o(\bar{T}(r_o) - T^*(r)) - \frac{1}{2}\tau_{rr} \quad (2.3)$$

where the dimensionless temperature $T^* = T(r)/\Delta T$, and the dimensionless average temperature in the shell between r_i and r is denoted by $\bar{T}(r)$. Thus

$$\bar{T}(r) = (3 \int_{r_i}^r r^2 T^* dr) / (r^3 - r_i^3) \quad (2.4)$$

If the crucible is initially at some uniform temperature T_a , and its inner surface is suddenly raised to $T_a + \Delta T$ the temperature distribution in the crucible corresponds to

$$T^* = 1.0 - (1/r^*) \sum_{N=1}^{\infty} A_N \sin(p_N[r^*-1]) \exp(-p_N^2 t/t_k) \quad (2.5)$$

where $r^* = r/r_i$, $t_k = r_i^2/\kappa$, the p_N are the positive roots of $\tan(p_N(r_o^* - 1)) = r_o^* p_N$ and the A_N are constants depending on p_N and r_o^* . Here $r_o^* = r_o/r_i$. The resulting radial stress is compressive throughout the shell whereas the tangential stress although compressive adjacent to the hot inner surface is tensile beyond some radius which varies with time. (These are shown in fig 2 when $r_o^* = 2$). Although the compressive stresses are larger, rocks are much weaker in tension, thus the relevant failure criterion is that the tangential tensile stress exceeds the tensile strength. Figure 3 shows the locus of the maximum tensile tangential stress as a function of time. For $r_o^* = 2$, the maximum value of $\tau_{\theta\theta} = 0.18\tau_o$. This may be compared with $0.28\tau_o$ for a constant heat flow produced by an applied temperature difference ΔT .

For basalt, $\kappa = 8.4 \times 10^{-7} \text{ m}^2/\text{s}$; hence for a 2m pool, $t_k = 5.10^6 \text{ sec}$. From figure 3, times of order 10^4 s are required (when $r_o^* = 2$) to reach tensile tangential stresses of $0.05\tau_o$ some 0.3m beyond the inner radius. If $T=500\text{K}$ such a stress would be comparable with the tensile strength of basalt.

For thicker walled crucibles, the maximum tensile stress is lower (see figure 3 for $r_o^* = 5$). Overall if the rock or concrete basemat behaves as a true continuum then significant cracking from failure in tension seems unlikely.

If the bed is composed of blocks, then the possibility of further crack production requires a more localized analysis. Let a typical block dimension be $2r_o$; then we consider a sphere of radius r_o , which has a sudden temperature increase applied at its surface. If fracture results in a sphere, then the localized stress concentrations in other shapes can but enhance the effect. Chen et al. [4] have carried out experiments in which a 10cm diameter sphere of Dresser basalt was heated to a surface temperature of 600C in 35 sec by a radiative flux of $\sim 80 \text{ kW/m}^2$ applied to the surface. Only half the surface was heated; the other half was insulated. This experiment is relevant to the arrival of hot pool material on one side of a block. Detailed calculations were

carried out by Chen et al. which predicted a maximum tensile tangential stress of about $4 \times 10^7 \text{ N/m}^2$, some 0.02m below the surface. The fragments which were produced in their experiments were of this order of magnitude. The formulae for the tangential stress in the analysis of Chen et al. do not scale in a straightforward fashion, but we note that the maximum tensile stress was generated on the radius normal to the plane separating heated and insulated hemispheres. This suggests that a spherically symmetric analysis will give reasonable estimates of the maximum radial and tangential stresses. When a spherically symmetric radial temperature distribution is present in a sphere of radius r_0 the radial and tangential stresses are given ([3]p418) by (2.2) and (2.3), with $r_i=0$ in (2.2) and (2.4). If the sphere is initially at T_a , and its surface temperature is suddenly raised to $T_a + \Delta T$, then the resulting temperature $T(r,t)$ within the sphere can be expressed as $(\Delta T) \cdot (r_0/r) \cdot h(r,t)$ where h is an infinite sum of error functions (see [5] p233); at the centre of the sphere a uniform tension is generated which has its maximum value $0.38 \tau_0$ when $\kappa t/r_0^2 = 0.06$ [6]. This temperature profile consists mainly of a steep boundary layer adjacent to the outer surface, while $\kappa t \ll r_0^2$. Such a temperature profile can be approximated by the piece-wise linear form

$$\begin{aligned} T^* &= 0 & \text{for } r \leq R \\ &= (r-R)/(r_0-R) & \text{for } R \leq r \leq r_0 \end{aligned} \quad (2.6)$$

Fig 4b shows the corresponding average (dimensionless) temperature $\bar{T}(r)$, the radial stress τ_{rr} and the tangential stress $\tau_{\theta\theta}$ when $\epsilon \equiv R/r_0$ is 0.6. If $B \equiv (1 + \epsilon + \epsilon^2 + \epsilon^3)/4$, then $\bar{T}(r_0) = 1 - B$ where clearly $B \leq 1$. The maximum tensile tangential stress is equal to $(2/3) \tau_0 \bar{T}(r_0) = (2/3) \tau_0 (1-B) \equiv \tau_{\max}$ and the tangential stress has this value for $r \leq R$. The radial stress is always tensile, and has its maximum value (also τ_{\max}) for $r \leq R$. Beyond $r = R$ the tangential stress is essentially linear, and at $r=r_0$, $\tau_{\theta\theta} = -B \cdot \tau_0$.

Fig.4a shows the temperature profile and the radial and tangential stresses calculated by Chen et al. for the radius normal to the plane separating heated and insulated hemispherical surfaces of a basalt sphere; these are after a time $0.05 r_0^2 / \kappa$. The qualitative agreement between the results of Chen et al. and those from the simple spherical model considered above are good, and $(1.25 \pm 0.25) \tau_{\max}$ appears to be a good estimate of the maximum tensile stress generated tangentially for the one sided heating case.

Since a linear profile is only appropriate when the boundary layer is reasonably thin, then $B = 1 - 3\beta/2$ when $\beta \equiv (1-\epsilon)$ is $\ll 1$. Thus in the spherical case, with the boundary layer temperature profile, then $\tau_{\max} = \tau_0 \cdot \beta$, or

$$\max(\tau_{\theta\theta}) = \frac{E\alpha\Delta T}{1-\nu} \left(\frac{r_0 - R}{r_0} \right) \quad (2.7)$$

We see that τ_{\max} is (i) proportional to ΔT , (ii) proportional to the boundary layer thickness $\delta \equiv r_0 - R$ and (iii) inversely proportional to the dimension of the sphere r_0 .

For basalt with $T=1000\text{K}$, $\tau_0 = 1.3 \times 10^9 \text{ N/m}^2$. Then τ_{\max} will exceed the tensile strength of 3.10^7 N/m^2 provided δ/r_0 exceeds $1/40$. If $r_0 = 0.15\text{m}$, then provided the

boundary layer is more than a few millimetres thick, fracture is likely to occur. Thus 1 foot cube blocks of basalt can be expected to break-up into centimetre size fragments ; the fissures will however be hair-line cracks unless the cracks are widened by the passage of vapour.

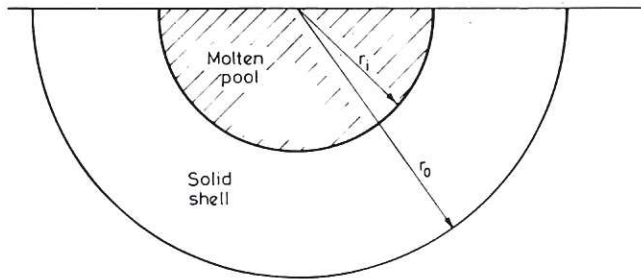


Fig.1. A solid crucible of outer radius r_o and inner radius r_i containing a molten pool

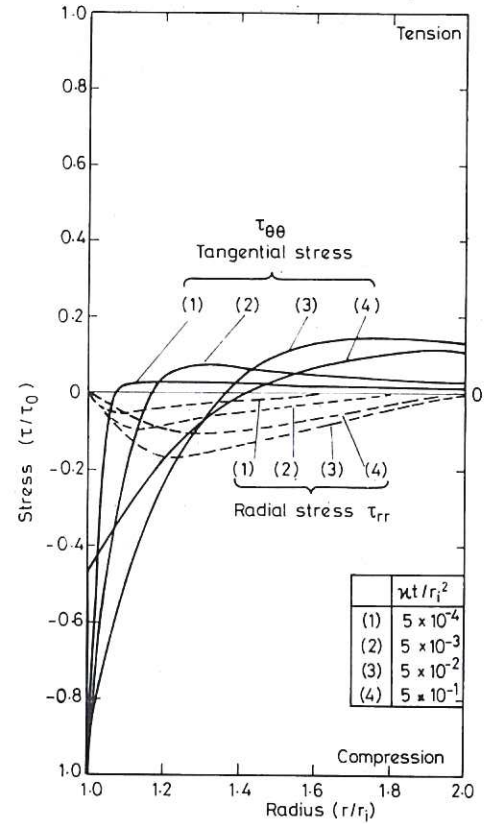


Fig.2. Tangential stresses $\tau_{\theta\theta}$ and radial stresses τ_{rr} induced in a spherical shell for which $r_o/r_i=2$ at the times indicated after the temperature of the inner surface is raised by ΔT .

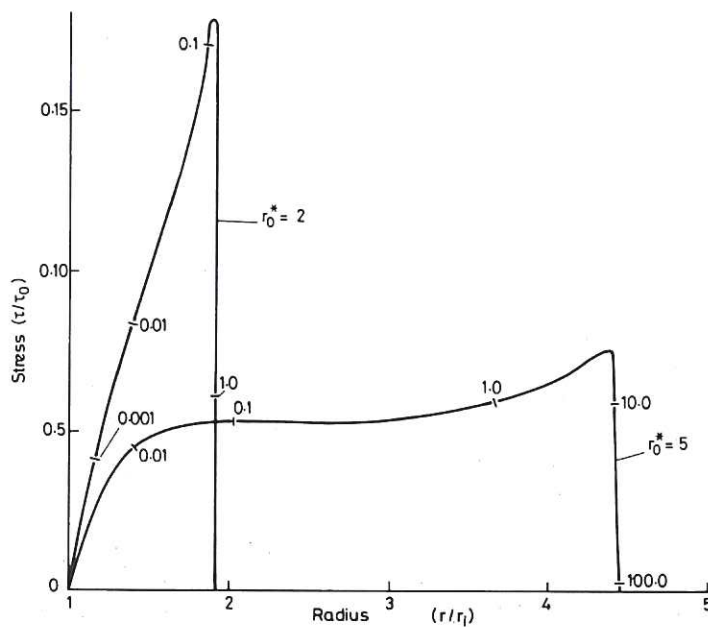


Fig.3. Locus and magnitude of the maximum tensile tangential stress in spherical shells with $r_o/r_i=2$ and $r_o/r_i=5$. The non-dimensional time t/t_κ after the inner surface temperature is raised by ΔT is indicated on both loci.

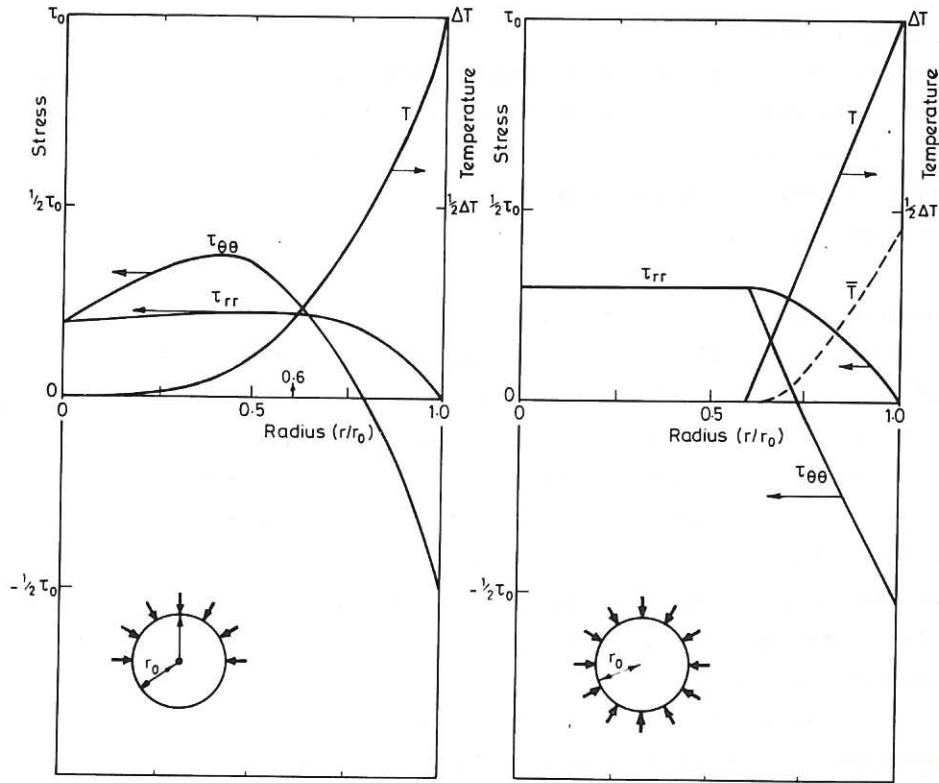


Fig.4. The temperature and corresponding stress profiles in a solid sphere of radius r_0 (i) on the vertical radius at $t=0.05 r_0^2/\kappa$ when the upper surface is radiantly heated uniformly and the lower surface is insulated (from [4]) (ii) for a spherically symmetric configuration containing a linear temperature profile $T(r)$ for $r>0.6r_0$. The average temperature $\bar{T}(r)$ is also indicated.

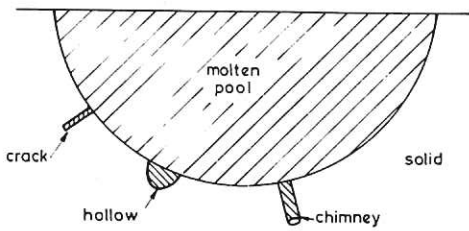


Fig.5. A molten pool of core debris diluted by bed material is shown encountering a plane sided crack, a cylindrical chimney crack, and a hemispherical hollow within the solid substrate.

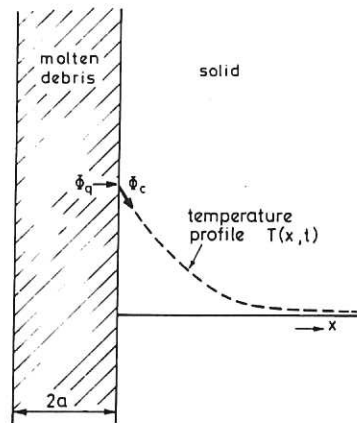


Fig.6. An isolated plane crack of width $2a$, containing molten core debris close to the melting point of the bed. ϕ_q is the heat flux density to the crack wall; ϕ_c is the conductive flux away from it into the bed.

3. THE MELTING OF FISSURES

We now suppose that the bed contains cracks, fissures and holes into which molten core debris can penetrate ahead of the melting front of the growing pool. In this section we consider whether debris entering a gap or crack ahead of the melting front will freeze or cause the gap to expand by further melting, possibly opening up new pathways through the bed.

3.1 Formulation

Three geometries are considered - a parallel sided crack, a cylindrical tube or shaft, and a hemispherical hollow. Simple criteria may be found by using solutions for the flow of heat into an external ambient medium from the surface of a slab, cylinder or sphere, which has suffered a step change in temperature corresponding to the sudden arrival of the molten debris in the fissure (fig.5). This determines the maximum rate at which heat may be removed from the debris without melting the ambient material. We will assume that all the decay heat is generated within the debris, which gives a conservative (over) estimate as the γ radiation component has a typical range of a few centimetres. It is also assumed that the debris, which may have been diluted by molten sacrificial material, is close to the melting point of the sacrificial material.

Consider first a parallel sided crack. If a plane surface is suddenly raised at time $t=t_0$ to a temperature θ_m in a semi-infinite medium at ambient temperature θ_a , and the surface temperature is then maintained, it may be shown for this text book problem ([5]p60) that the heat flux density at $x = 0$ at subsequent times is

$$\phi_c = k(\theta_m - \theta_a) / \sqrt{\pi k(t-t_0)} \quad (3.1)$$

This result is now applied to the situation arising when heat-producing debris is introduced into a slab-shaped gap (fig 6). If no melting is to occur then the surface temperature must remain below θ_m ; thus equation (3.1) gives a maximum value of the heat flux density that can be removed without melting occurring. If in the initial stages the surface temperature increases gradually rather than as step function, (3.1) gives a lower bound and so is conservative. If the decay heat flux density ϕ_q exceeds ϕ_c , melting would occur; if it is less, then some of the debris will freeze.

For a plane crack of width $2a$ containing molten core debris (power density $q(t)$),

$$\phi_q = aq(t) = aQ_0 f(t) / \chi(t_0) V_0 \quad (3.2)$$

where (Q_0/V_0) is the power density on stream, $f(t)$ is the decay heat function and $\chi(t)$ is the factor by which the molten core debris has been diluted by sacrificial material. If $R \equiv \phi_c / \phi_q$ is the 'flux ratio' then the criterion for no melting to occur in a crack of given dimension is

$$R \geq 1 \quad (3.3)$$

Defining $\alpha \equiv k(\theta_m - \theta_0)V_0/Q_0$ and $s_1 \equiv \sqrt{(t-t_0)}/a$, then R can be written as

$$R = \alpha \chi(t_0) F(s_1) / a^2 f(t) \quad (3.4)$$

For a parallel sided crack

$$F(s_1) = (\pi s_1)^{-\frac{1}{2}} \quad (3.5a)$$

If a similar analysis is carried out for molten debris entering suddenly, at $t=t_0$, a cylindrical chimney-like crack of radius a , or a hemispherical hollow of radius a , the same criterion (3.3) is found for no melting, where however $F(s_1)$ in (3.4) is defined for the cylindrical tube by

$$F(s_1) = 2G(s_1) \quad (3.5b)$$

and for the hemispherical hollow by

$$F(s_1) = 3(1 + (\pi s_1)^{-1/2}) \quad (3.5c)$$

The Jaeger integral $G(s)$ is defined by ([5] p 336)

$$G(s) = (4/\pi^2) \int_0^\infty e^{-su^2} \left\{ u(J_0^2(u) + Y_0^2(u)) \right\} du \quad (3.6)$$

where J_0 and Y_0 are solutions of the zero order Bessel equation. Expansions of G for small and large s are given in [5] and are tabulated in table 1. Fig 7 shows $F(s)$ for the three cases (3.5a,b,c).

3.2 Minimum Fissure Dimensions

Equation (3.3) gives implicitly the critical size of fissure below which a fissure will not melt. However it represents a dynamic criterion with the critical size varying as a function of t . If a fissure of dimension a is not to be enlarged by melting then equation (3.3) must hold for all $t \geq t_0$. Hence we require the largest value of a for which $R \geq 1$ for all $t \geq t_0$, to obtain a criterion independent of t .

Let the decay heat function have the mildly conservative form [7]

$$f(t) = f_0 (t^{-1/4} - [t + t_q]^{-1/4}) \quad (3.7)$$

where t_q is the irradiation time for the fuel on stream.

Define the dimensionless parameter $P(t_0)$ by the following ratio of enthalpies:

$$P(t_0) \equiv \rho c (\theta_m - \theta_a) V_0 \chi(t_0) / (Q_0 f_0 t_q^{3/4}) \quad (3.8)$$

The numerator is the sensible heat in the diluted debris; the denominator is essentially the total integrated decay heat $Q_0 \tau(\infty)$ when f is given by (3.7).

Thus $P \leq 1$.

It is convenient to non-dimensionalize the various times with respect to the thermal diffusion time $t_k \equiv a^2/\kappa$, and write $s = t/t_k$, $s_q = t_q/t_k$, $s = t_0/t_k$, and $s_1 \equiv (t - t_0)/t_k$.

Then R can be written as $(s_q/\pi)^{1/2} P(t_0) H(s)$ where

$$H(s) = (\pi^2 s s_q)^{1/2} F(s_1) / (1 - \lambda) \quad (3.9)$$

in which $\lambda^4 \equiv t/(t + t_q) = s/(s + s_q)$. $H(s)$ is the only factor of R which depends on t . The form of H is sketched in fig 8, and it clearly has a single minimum value H_{\min} , when $t = t_{\min}$ (say). If $t_{\min} \gg t_0$, one can show that H_{\min} is given approximately by

$$\left. \begin{aligned} H_{\min} &= 4 & \text{Plane} \\ &= 8 + 4 C (\pi s_q)^{1/2} & \text{Cylindrical} \\ &= 12 + 6 (\pi s_q)^{1/2} & \text{Spherical} \end{aligned} \right\} \quad (3.10)$$

where $C \approx 1$. In the plane case $t_{\min} = t_q/(12.8)$ for all s_q (this corresponds to $\lambda = \lambda_0 \approx 0.5188$). This is also the critical time if $s_q \ll 1$ for the cylindrical and spherical geometries. When $s_q \gg 1$, the time when H achieves its minimum is given by $(s/F(s_1))(dF(s_1)/ds) = -1/4$ for cylindrical and spherical geometries; as fig 7 indicates this corresponds, when

$t_{\min} \gg t_0$, to $t_{\min} = a^2/\pi\kappa$ for spheres and $t_{\min} = 4a^2/\kappa$ for cylinders. Fig. 9 shows the dependence of H_{\min} and t_{\min} on s_q for the spherical case when $t_{\min} \gg t_0$; the cylindrical

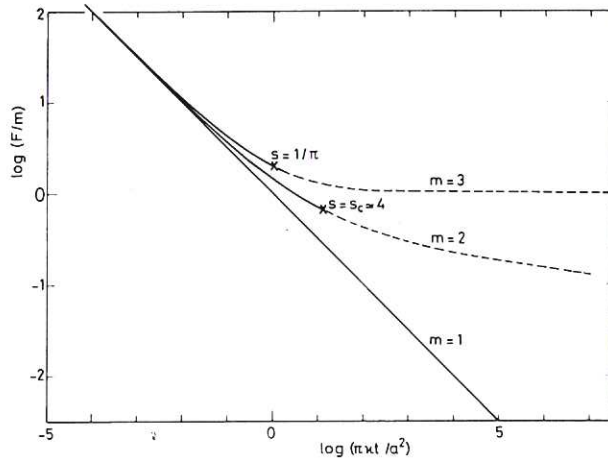


Fig. 7. The dimensionless conductive heat flux density $F/m \equiv \phi_c/k(\theta_m - \theta_a)$ at the wall of a crack; $m=1$ (plane), $= 2$ (cylindrical), $= 3$ (spherical). The critical time t_{min} at which a crack of dimension a is closest to melting always lies on the solid parts of the curves. If the irradiation time $t_q \gg t_k$ then t_{min} tends to t_k/π (spheres) and $\approx 4t_k$ (cylinders), corresponding to $s=\pi^{-1}$ and $s \approx 4$ respectively.

s	G(s)	
0.01	6.13	Small s expansion
0.03	3.74	
0.1	2.25	
0.3	1.45	
1.0	1.00	exact
3	0.85	large s expansion
10	0.61	
30	0.46	
100	0.36	
10^3	0.26	
10^4	0.20	
10^5	0.16	
10^6	0.14	

Table 1. The dimensionless heat flux density $G(s)$ for the diffusion of heat from a cylindrical shell at constant temperature

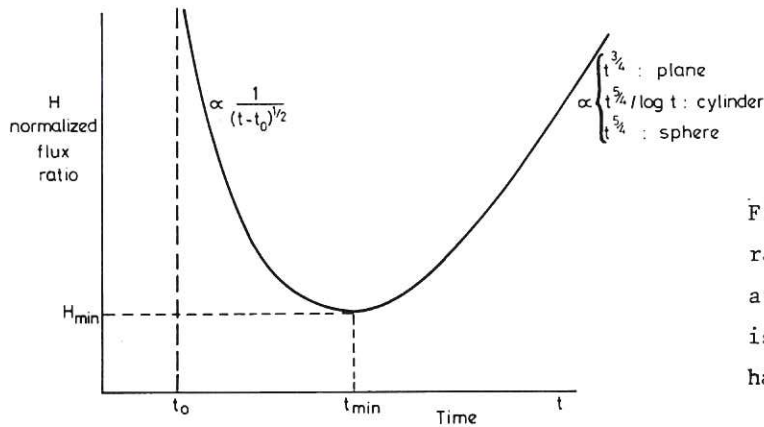
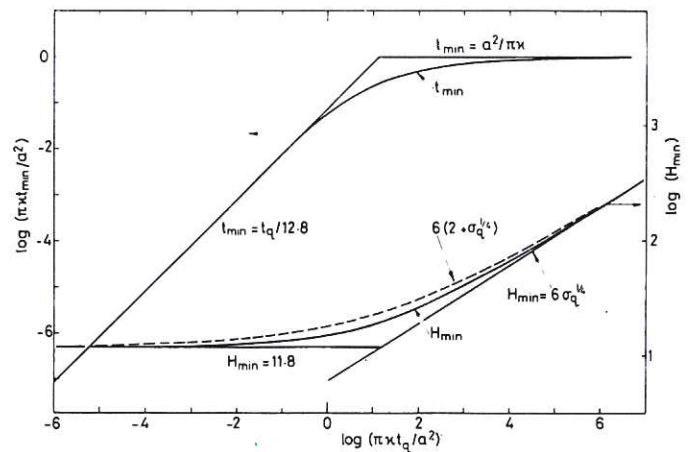


Fig.8. A sketch of the normalized flux ratio H given by (3.9); t_0 is the time at which the debris enters the crack, t_{min} is the time at which H (and thus ϕ_c/ϕ_q) has its minimum value.

Fig.9. The dependence of H_{min} , the minimum value of H , on t_q/t_k for the spherical case when $t_{min} \gg t_0$; the corresponding t_{min} is also shown. There are two regimes, corresponding to $t_q \geq t_k$



case is similar.

To confirm the conservative nature of the assumption that $t_{\min} \gg t_o$, so that s_1 may be replaced by s in calculating an overall minimum of H , H has been calculated in the slab case as a function of (t/t_q) for a range of values of t_o . Fig. 10 shows clearly that the overall minimum of H viz 3.93 occurs when t_o tends to zero and $t_{\min} = t_q/12.8$.

A sufficient condition for no melting is thus $R_{\min} \geq 1$ where

$$R_{\min} = (s_q/\pi)^{1/2} H_{\min}(s_q) P(t_o) \quad (3.11)$$

in which $H_{\min}(s_q)$ is given by (3.10) and $P(t_o)$ by (3.8). Fig. 11 shows $Z \equiv \pi R_{\min}/4P(t_o)$ for the three geometries.

Since P is necessarily ≤ 1 , only the solid parts of the curves corresponding to $Z \geq 1$ are relevant.

Thus the critical fissure size a_{crit} by

$$\begin{aligned} a_{\text{crit}}/\sqrt{\pi \kappa t_q} &= 4P/\pi \\ &= (4P/\pi)^{2/3} (1 + 2(4P/\pi)^{1/3} + \dots) \\ &= (6P/\pi)^{2/3} (1 + 2(6P/\pi)^{1/3} + \dots) \end{aligned} \quad (3.12)$$

for plane crack, cylindrical chimney, and hemispherical hollow respectively, for $P \ll 1$. Note that a_{crit} is proportional to P for plane cracks, and proportional to $P^{2/3}$ for cylinders and spheres when $P \ll 1$.

3.3 Effects of Dilution

To calculate a numerical value for a_{crit} , P must be evaluated. If the core debris is diluted by sacrificial material, so that the resultant molten pool is close to its melting point, then

$$\rho(L + c \Delta T) V_o \chi(t) = \Gamma Q_o \tau(t) \quad (3.13)$$

where $\chi(t)$ is the dilution factor achieved up to time t . The coefficient Γ is the fraction of the decay heat generated up to time t which is stored in the molten pool; clearly $\Gamma \leq 1$. From (3.13), P can be expressed as $B\Gamma\tau(t_o)/\tau(\infty)$ where $B = 4S/\{3(1+S)\}$ is at most of order unity. For common refractory materials $S \approx 2$ so that $B \approx 1$.

When the melting front of the main pool is advancing rapidly, so that thermal front thickness is small, then $\tau(t) \sim \frac{4}{3} f_o t^{3/2}$ if f has the form given by (3.7). This regime is appropriate to the analysis earlier, where it is assumed that the arrival of the debris in the fissure is sudden and the rock is still at ambient temperature. It follows that (neglecting a factor of order unity)

$$P(t_o) = \Gamma \cdot (t_o/t_q)^{3/2} \quad (3.14)$$

Combining this with (3.12), we obtain for plane cracks

$$a_{\text{crit}} \approx 2\sqrt{\kappa t_q} (t_o/t_q)^{3/4} \Gamma \quad (3.15a)$$

and

$$a_{\text{crit}} = \epsilon \sqrt{\kappa t_o} \Gamma^{2/3} \quad (3.15b,c)$$

for cylinders and hemispheres where

$$\epsilon \sim 2(\text{cylinders}) \text{ and } \epsilon \sim 3(\text{spheres}) \quad (3.16)$$

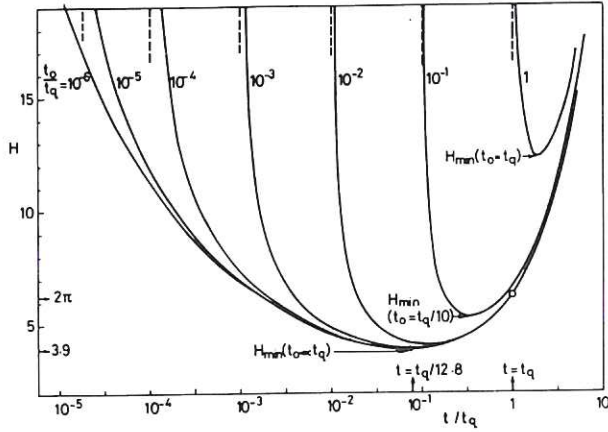


Fig.10. The time dependence for a plane crack of the normalized flux ratio H for various values of t_0/t_q . When $t_0 \ll t_q$, $H_{\min} = 3.9$, and the corresponding critical time $t_{\min} = t_q/12.8$.

A typical value for κ is $10^{-6} \text{ m}^2/\text{s}$. If the pool has poor heat transfer to any overlying coolant, then $\Gamma \sim 1$. If $t_q \sim 10^7 \text{ sec}$ and $t_0 > 10^3 \text{ sec}$ (a modest requirement) then $a_{\text{crit}} \sim 6 \text{ mm}$ [plane], $\sim 6 \text{ cm}$ [cylinder] and $\sim 9 \text{ cm}$ (sphere).

If the molten pool is formed in such a way that good heat transfer paths exist up to the overlying sodium (in the case of an LMFBR), then Γ will be much smaller. Accurate calculations for the critical radius of a cylindrical fissure have been carried out using (3.4), with $\alpha = 1.1 \times 10^{-6} \text{ m}^2/\text{s}$, $\kappa = 10^{-6} \text{ m}^2/\text{s}$, the decay heat function $f(t)$ based on the FISPIN data [8], and the dilution factor $\chi(t_0)$ chosen to be typical of those found in melt-pool simulations using PAMPUR [1]. Table 2 shows a set of results from these calculations. The agreement between the tabulated results and the calculated value (3.16) is very satisfactory; $\epsilon = 2$ is clearly a good approximation over a wide range of t_0 .

The critical fissure size scales as χ for plane cracks and as $\chi^{2/3}$ for chimneys and hollows. It is the increase of the dilution factor with time which is responsible for the fact that the critical size for fissures is greater at later times.

The criteria (3.15) provide a basis for determining how closely packed a sacrificial bed must be for it to function in the manner envisaged.

t_0 (s)	χ	a_{crit} (m)	t_{\min} (s)	Γ	ϵ
3.2×10^3	3	0.018	1.5×10^4	0.09	1.58
10^4	9	0.039	5.2×10^4	0.12	1.60
3.2×10^4	20	0.068	1.5×10^5	0.117	1.60
10^5	40	0.114	2.7×10^5	0.106	1.60
3.2×10^5	80	0.225	7.0×10^5	0.099	1.86
10^6	140	0.410	2.2×10^6	0.086	2.10
3.2×10^6	200	0.646	6.8×10^6	0.066	2.20
10^7	200	0.797	1.8×10^7	0.040	2.16

Table 2. Critical radii for cylindrical cracks. If the radius is less than a_{crit} the sides of the crack will not melt. The dilution factor χ is chosen to be reasonably realistic for diluted debris entering the crack at time t_0 . coefficients Γ and ϵ are defined in (3.13) and (3.15).

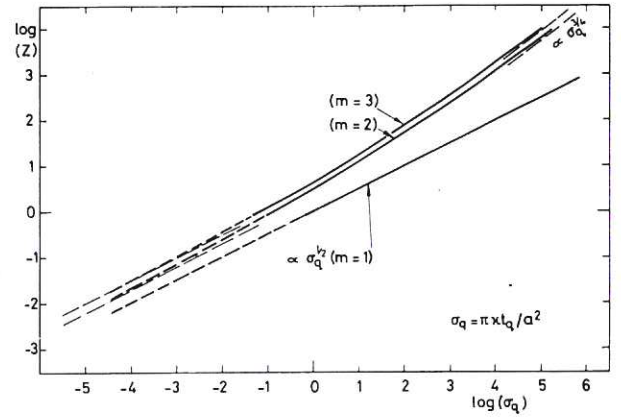


Fig.11. The function $Z \equiv \pi R_{\min}/4P(t_0)$ as a function of $\pi t_0/t_q$ for plane ($m=1$), cylindrical ($m=2$), and hemispherical ($m=3$) cracks. A sufficient condition for no melting is $Z > \pi/4P(t_0)$.

4. CONCLUSIONS

(i) If a sacrificial bed is composed of lumps of dimension D and tensile strength σ_t , then a criterion for cracking when a temperature difference ΔT is applied in a boundary layer of thickness δ is

$$\frac{2 E \alpha \Delta T}{1 - \nu} \frac{\delta}{D} \geq \sigma_t$$

This assumes elastic behaviour. Non-linearity in the stress-strain law will increase the required ΔT , stress concentration may reduce it.

(ii) The criterion for a crack of width $2a$ not be enlarged by melting when entered by molten, diluted core debris at time t_0 after shutdown is

$$a < a_{crit}$$

where a_{crit} is given by (3.15). Typically the critical size of plane sided cracks is an order of magnitude smaller than the critical size of cylindrical chimneys or hemispherical hollows.

Acknowledgments This work was carried out with the support of the U.K. Safety and Reliability Directorate Culcheth.

REFERENCES

- [1] Peckover R S, Turland B D and Whipple R T P (1977) On the Growth of Melting Pools in Sacrificial Materials in Proc. Third Post Accident Heat Removal Conference, Argonne Nov. 1977. (ANL-78-10)
- [2] Turland B D, Peckover R S and Dullforce T A (1977) On the Stability of Advancing Melting Fronts to Spatial Perturbations in Proc. Third Post Accident Heat Removal Conference, Argonne Nov. 1977 (ANL-78-10)
- [3] Timoshenko S and Goodier J N (1951) Theory of Elasticity 2nd Edition
- [4] Chen T S, Thirumalai K and Cheung J B (1974) Transient Temperature and Thermal Stresses in a Sphere due to arbitrary local heating followed by cooling. A.S.M.E. (Heat Transfer) paper 73-WA/HT-5.
- [5] Carslaw H S and Jaeger J C (1959) Conduction of heat in solids 2nd Edition Oxford
- [6] Grünberg G (1925) Z. Physik 35, 548 (cited in [3])
- [7] Peckover R S (1978) Thermal moving boundary problems arising in reactor safety studies. Paper presented at Durham symposium on free and moving boundary problems in heat flow and diffusion (Culham Laboratory Preprint CLM-P562)
- [8] Turland B D and Peckover R S (1977) The Distribution of Fission Product Decay Heat in Proc. Third Post Accident Heat Removal Conference, Argonne Nov. 1977 (ANL-78-10)

